Published in final edited form as:
Mol Pharm. 2010 August 2; 7(4): 1283–1290. doi:10.1021/mp100073s.

Silencing Heat Shock Protein 27 (Hsp27) decreases metastatic behavior of human head and neck squamous cell cancer cells in vitro

Zhenkun Zhu[1,2], **Xin Xu**[2,*], **Yanke Yu**[1], **Martin Graham**[3], **Gangli Liu**[2], **Mark E. Prince**[3], **Thomas E. Carey**[3,*], and **Duxin Sun**[1,*]

[1]Department of Pharmaceutical Sciences, College of Pharmacy, University of Michigan, Ann Arbor, MI, USA 48109

[2]College of Stomatology, key lab of Oral Biomedicine of Shandong Province, Shandong University, Jinan, P.R.China, 250012

[3]Department of Otolaryngology, University of Michigan, Ann Arbor, MI, USA 48109

Abstract

The small heat shock protein 27 (Hsp27) is a molecular chaperone that is involved in a variety of cellular functions in cancer cells. The purpose of this research is to study Hsp27 in vitro metastatic behaviors of head and neck squamous cell carcinoma cells (HNSCC). The expression of Hsp27 in primary and metastatic cell lines derived from the primary HNSCC and a synchronous lymph node metastasis in the same patient was determined using real-time PCR and western blotting. Proliferation of the primary and metastatic HNSCC cell lines was evaluated using the MTS proliferation assay. Metastatic behavior was assessed using migration and invasion assays. SiRNA knockdown of Hsp27 was performed in the highly migratory metastatic HNSCC cell line. MTS assays showed that the primary (UM-SCC-22A) and metastatic (UM-SCC-22B) HNSCC have similar proliferation rates. However, UM-SCC-22B derived from the metastasis showed 2.3 to 3.6-fold higher migration ability and 2-fold higher invasion ability than UM-SCC-22A. Real-time PCR demonstrated that Hsp27 mRNA is 22.4-fold higher in metastatic UM-SCC-22B than primary UM-SCC-22A. Similarly, Western blotting showed that Hsp27 is rarely detectable in UM-SCC-22A whereas UM-SCC-22B expresses a 25-fold higher level of Hsp27 protein. SiRNA-mediated knock down of Hsp27 in UM-SCC-22B reduced Hsp27 mRNA expression by nearly 6 - fold and protein expression by 23-fold. Furthermore, siRNA knockdown of Hsp27 decreased metastatic behaviors of UM-SCC-22B by 3 to 4-fold in migration and 2-fold in cell invasion reducing cell invasion and migration to levels similar to the primary HNSCC UM-SCC-22A. These data indicate that Hsp27 may regulate metastatic potential of HNSCC cancer cells. Targeting Hsp27 may decrease metastasis in head and neck squamous cell cancer cells.

Keywords

Heat Shock Protein 27; human head and neck squamous cell cancer; metastasis; siRNA

[*]To whom correspondence should be addressed: Duxin Sun, Ph.D., Associate Professor, Department of Pharmaceutical Sciences, College of Pharmacy, University of Michigan, Room 2020, 428 Church Street, Ann Arbor, MI, USA 48109, Tel: 734-615-8740 (Office); 734-615-8851 (Lab)Fax: 734-615-6162; duxins@umich.edu, Xin Xu, Ph.D, Professor, College of Stomatology, Shandong University, Room 511, 44-1 Wenhuaxi Road, Jinan, Shandong Province, P.R.China, 250012, Tel: +86 531 883 82636(Office); xinxu@sdu.edu.cn, Thomas Carey, PhD, Professor, Department of Otolaryngology, University of Michigan, Room 5311 Medical Sciences I, 1150 West Medical Center Drive, Ann Arbor, MI, USA 48109-5616, Tel: 734-764-4371 (Office); fax: 734-764-0014, careyte@umich.edu.

Introduction

Head and neck squamous cell carcinoma (HNSCC) is the 6th most prevalent cancer types worldwide with an incidence of more than 500,000 cases annually and a high mortality rate, making it the fifth leading cause of cancer related death 1. In the United States, it accounts for 6% of all cancer diagnoses and results in an estimated 14,000 deaths annually 2. Despite the advanced therapeutic regimens used in treating HNSCC, oral cavity cancer survival during 1996–2003 was less than 50% on average according to the data from American Cancer Society. Furthermore, patients with recurrent or metastatic HNSCC have median survival of approximately 6 months 1, 2. The major contributing factors for low survival include local-regional relapse, lymph node or distant metastatic spread of the primary tumor 3, 4.

Tumor progression to the invasive and metastatic stage represents the most ominous challenges in the management of HNSCC. Metastasis of HNSCC is a complex process associated with multiple biochemical and genetic changes. Increased cell motility and invasive growth are considered to be important in the metastatic cascade. Degradation of extracellular matrix and tumor angiogenesis may also contribute to HNSCC metastasis. Several proteins have been studied in HNSCC metastatic disease such as Hsp90, HER2 5, MMP2 6, 7, MMP9 7,TGF-β1 8. However, the actual mechanisms driving metastasis of HNSCC remain unclear.

Recent studies suggest that high levels of heat shock proteins (HSPs) and heat shock factor 1 (HSF1) that regulates HSP expression promote prostate adenocarcinoma tumor cells to invade and to spread to distant organs 9, 10. Clinical studies showed a high correlation between HSF1 overexpression and HSPs including Hsp27 and Hsp70 which have also been shown to be correlated with invasion and/or metastasis of prostate cancer 10–12.

Hsp27 acts as a molecular chaperone in cellular responses for a variety of stresses such as heat shock, toxicants, and oxidative stress 13. Hsp27 has also been shown to have various functions in signal transduction, regulation of growth, differentiation, and tumorigenesis. High levels of Hsp27 have been found in prostate cancer 14, human hepatocellular carcinoma 15, 16, renal cell carcinoma 17, oral tongue squamous cell carcinoma 18, and breast cancer 19. Garrido, et al. overexpressed Hsp27 in REG colon cancer cells and increased REG cell tumorigenicity in the syngeneic host 20, 21. Furthermore, overexpression of Hsp27 has also been linked to the metastasis of several tumor types including prostate cancer 14, hepatocellular cancer 15, tongue squamous cell cancer 18. For example, High level of hsp27 expression was associated with tongue squamous cell cancer invasion and metastasis 22. Curiously, Masanobu et al. showed that patients with Hsp27-negative esophageal squamous cell carcinoma tended to have a poorer prognosis compared with patients with Hsp27-positive tumors 23. The function of Hsp27 in head and neck squamous cell cancer has not been fully understood.

We observed that Hsp27 was overexpressed in a head and neck squamous cell carcinoma from a metastatic lymph node, but rarely expressed in the primary cancer cells from the same patient. We hypothesize that Hsp27 potentially may be involved in the metastasis of head and neck squamous cell carcinoma cells (HNSCC). These head and neck squamous cancer cell lines served as paired controls to study Hsp27 function. We first studied the expression level of Hsp27 in both metastatic and primary head and neck squamous cell cancer cells, then we correlated the expression levels of Hsp27 to cell motility and invasion. siRNA was used to knockdown Hsp27 in metastatic head and neck squamous cell carcinoma cells to study its function in metastasis.

Material and Methods

Materials and Cell culture

UM-SCC-22A and UM-SCC-22B cells were isolated from a head and neck cancer patient who presented with synchronous primary and metastatic to the head and neck cancer program at the University of Michigan. The primary head and neck squamous cancer cells (UM-SCC-22A) were obtained from the surgical resection specimen of the primary cancer of the hypopharynx, while the metastatic head and neck squamous cancer cell line (UM-SCC-22B) was established from a metastatic lymph node of the same patient. This was an aggressive tumor that progressed and caused the death of the patient within 8 months of diagnosis. All cells were cultured in high Glucose Dulbecco's Modified Eagle's Medium (DMEM, Gibco-BRL, NY, USA) supplemented with 10% fetal calf serum, 2 mM L-glutamine, penicillin (100 units/ml) and streptomycin (100 μg/ml), and 100nM non-essential amino acids. Both cell lines were cultured at 37°C in a humidified atmosphere of 95% air and 5% CO_2.

MTS cell proliferation assay

Various numbers (10–5000) of UM-SCC22A and UM-SCC22B cells in 200ul DMEM/well supplemented with 10% fetal bovine serum were seeded to the wells of a 96-well plate, cultured for 24hr/48hr. The medium was allowed to equilibrate for 1 hour, then 25ul/well of combined MTS (3-(4,5-dimethylthiazol-2-yl)-5-(3-carboxymethoxyphenyl)-2-(4-sulfophenyl)-2H-tetrazolium, inner salt) / PMS (phenazine methosulfate) solution were added. After cultured at 37°C in a humidified 5% CO_2 atmosphere for 2.5hr. The absorbance at 490 nm was measured using Bio-Tek Elisa plate reader.

Real-Time PCR assay

RT-PCR was carried out as described previously 24. Briefly, TRIzol reagents (Invitrogen, Carlsbad, CA) were used to extract total cellular RNAs as described in protocol provided by manufacturer. Superscript III first strand synthesis kit from Invitrogen was used to reverse transcribe the cDNA. Then the real-time PCR is carried out in ABI PRISM 7900T real-time PCR system (Perkin-Elmer, Branchburg, NJ) using SYBR Green PCR Master Mix (Applied Biosystems, Foster City, CA). The primers used in RT-PCR are as follows: hsp27, forward, 5'-GTC CCT GGA TGT CAA CCA CT-3'; reverse, 5'-CTT TAC TTG GCG GCA GTC TAC-3'; Internal standard β-actin, forward, 5'-GCT CGT CGT CGA CAACGG CTC-3'; reverse, 5'-CAA ACA TGC TCT GGG TCA TCT TCT-3'.

mRNA levels were calculated as fold change compared to control. After completion of the RT-PCR, Ct values (cycle numbers in which signal intensity equal to the threshold value) will be obtained from the software. For each sample, ΔCt is calculated as $\Delta Ct = Ct_{hsp27} - Ct_{\beta\text{-actin}}$. Then ΔΔCt is calculated as $\Delta\Delta Ct = \Delta Ct_{treatment} - \Delta Ct_{control}$. The fold change of the hsp27 mRNA levels relative to control is calculated as $2^{-\Delta\Delta Ct}$

Western blot

The procedure for the Western blot analysis was briefly described as follows. Cells were washed twice with ice-cold PBS, collected in RIPA lysis buffer (Thermo Scientific, USA) supplemented with a protease inhibitor mixture (Sigma; added at a 1:100 dilution), and incubated on ice for 30 min. The lysate was then centrifuged at 14,000 × *g* for 15 min. Protein concentration was detected by BCA™ protein assay kit (Thermo Scientific, USA). Equal amounts of total protein were subjected to 20% SDS-PAGE electrophoresis, and proteins were transferred for 1 hr using a Bio-Rad Semi-Dry apparatus in a transfer buffer. The PVDF membranes were incubated in blocking buffer (0.01 M PBS, 0.05% Tween-20 with 5% nonfat dry milk) for 1 hr, probed with various antibodies against HSP27 (Cell

Signaling Technology, USA, 1:1000), Hsp90, Hsp70, Akt, cdk4, β-actin (Santa Cruz Biotecknology,1:1000) overnight at 4°C, and incubated with HRP-conjugated secondary antibody for 1hr at room temperature. Peroxidase activity on the PVDF membrane was visualized on X-ray film using ECL Western blotting detection system.

Small interfering RNA (siRNA) knock down of Hsp27

Gene silencing by small interfering RNA (siRNA) uses a small double-strand RNA that degrades target mRNA. HSP27 siRNA duplex that target the sequences as described previously 25 (sense: 5'- UGAGAGACUGCCGCCAAGUAA-3'; antisense: 5'-UUACUUGGCGGCAGUCUCAUU-3') were synthesized by Dharmacon (Lafayette, CO). Transfection of siRNA was carried using Lipofectamine 2000 (Invitrogen). Briefly, one day before transfection, cells were plated in 5 ml of growth medium without antibiotics. On the day of transfection, the media in 60-mm plates was replaced with 5ml of media without antibiotics and 1 ml of Lipofectamine 2000-siRNA complex. In 1ml of Lipofectamine 2000-siRNA complex, 10ul of Lipofectamine 2000 in 500 ul of Opti-Mem (Gibco) and 200 pmol siRNA in 500ul of Opti-Mem were mixed together for a final volume of 1ml. The mixture was incubated at room temperature for 20 min. In each 60-mm plate, the final siRNA concentration was 33 nM. The cells were incubated in a 37°C 5%CO_2 for 5hr. The media was replaced with 5 ml of media without antibiotics. Two controls (lipofectamine and scrambled siRNA) were included in the experiments 26. The scrambled siRNA (5'-AATTCTCCGAACGTGTCACGT-3') were purchased from Dharmacon (Lafayette, CO), this scrambled sequence does not match any human genome sequence). After 24–48 hr, the cells were collected to measure the mRNA and protein, or the cells were used in invasion and wound healing assays.

Cell migration assay

Cell migration ability was monitored using a wound-healing assay. Cells were seeded at a high density on 6-well cell culture plate. After serum-free incubation for 18 hr, wounds were made by scraping through the cell monolayer with a sterile micropipette tip. Cells were further incubated in cell culture medium for up to 72hr with or without siRNA transfection. Images were taken (×40) under the microscope to measure cell migration using the widths of wound in cell monolayer.

Cell invasion assay

The Matrigel-coated filter system (Becton Dickinson Labware, Bedford, MA, USA) was used to assess cell invasion. The Matrigel matrix is a reconstituted and solubilized basement membrane. The Matrigel invasion chambers have pore size of 8.0-um (1×10^5 pores/cm^2). Because the Matrigel matrix occludes the pores of the polyethylene terephthalate (PET) membrane, noninvasive cells are blocked from migrating through the membrane. The chambers were rehydrated with 500ul serum-free media for 2 hr at 37°C. After rehydration, the chambers were placed in the lower compartment, which was previously loaded with 680ul of cell culture medium with 10%FBS. The cells were placed in the upper chamber of the transwell with a density of 2×10^4 cells in cell culture medium with 1% FBS per 500ul per well. The cells were allowed to invade the Matrigel at 37°C in 5% CO_2 for 40 hr. Then the cells were fixed with cold methanol, and stained with 0.5% Crystal Violet for 10 min. Cells in the upper surface of filter were removed using a cotton swab and the cells that invaded through the Matrigel, which were located on the lower side of the filter were counted (8 fields/filter). Experiments were repeated three times. The invasived cells were counted under the microscope, and cells in 8 different view fields were counted along a line across the center point.

Results

Metastatic head and neck squamous cell carcinoma cells (HNSCC) showed higher invasion and migration, but similar proliferation ability compared to primary HNSCC

To determine the proliferation ability of metastatic Head and neck squamous cell carcinoma cancer cells (UM-SCC-22B) and primary cells (UM-SCC-22A), MTS assay was used to determine the number of viable cells in proliferation after 24 and 48 hr. When various cell numbers (10–5000 cells/well) were plated in cell culture plate, UM-SCC-22A and UM-SCC-22B showed similar growth rate after 24–48 hr culture ($P>0.05$) (Figure 1). These experiments indicate that the primary (UM-SCC-22A) and metastatic (UM-SCC-22B) head and neck cancer cells have similar proliferation rates.

Next, we tested the metastatic potential of the primary and metastatic head and neck cancer cell lines using in vitro invasion and in vitro migration assays. In the invasion assay, 2×10^4 cells were added to the upper chamber in culture medium containing 1%FBS with medium containing 10% FBS in lower chamber. At 40 hr, cells were fixed and stained, and then the cells on the lower surface of filter were counted under microscope (Fig.2a). Eight fields were counted in each plate and six experiments were conducted. The results showed that invading cell numbers of metastatic head and neck cancer cells UM-SCC-22B through matrigel were 53.56 ± 26.71 ($n = 6$), whereas the invading cells of primary head and neck cancer cells UM-SCC-22A through matrigel were 25.45 ± 14.57 ($n = 8$) (Fig.2b).

In the migration assay, a gap was generated in the cell layer using micropipette tip, then the cells were allowed to grow and migrate for 24, 36, and 48 hr (Fig.2c). After 24, 36, and 48 hr, the gap width of metastatic head and neck cancer cells UM-SCC-22B was reduced by $38.30 \pm 9.30\%$, $44.24\pm7.31\%$ and $66.50\pm14.36\%$, respectively. In contrast, after 24, 36, and 48 hr, the gap width of primary head and neck cancer cells UM-SCC-22A was remained unchanged and was reduced only by $16.85\pm2.81\%$, $15.61\pm3.17\%$ and $18.69\pm1.02\%$, respectively. These data showed that UM-SCC-22B migrate 2.3 to 3.6-fold faster than UM-SCC-22A (Fig.2d). These data suggest that metastatic head and neck squamous cell carcinoma cells (UM-SCC-22B) indeed showed higher metastatic potential although it has similar proliferation ability compared to primary head and neck squamous cell carcinoma cells UM-SCC-22A.

Hsp27 mRNA and protein levels are higher in metastatic head and neck squamous cell carcinoma cells (HNSCC)

To investigate the expression of several heat shock proteins and oncogenic proteins in primary and metastatic head and neck squamous cell carcinoma cells (UM-SCC-22A and UM-SCC-22B), we used western blotting to detect the level of Hsp90, Hsp70, and Hsp27, AKT, and Cdk4. The results revealed that hsp27 protein level was rarely detectable in primary UM-SCC-22A cells, while metastatic UM-SCC-22B showed 25.3-fold higher Hsp27 protein expression than UM-SCC-22A (Fig. 3a). In comparison, we also monitored the expression levels of other chaperones (Hsp90 and Hsp70) and a few other oncogenic proteins (AKT, cdk4). The western blotting result showed similar levels of these proteins in these two cells lines. To confirm the different expression levels of Hsp27 in two head and neck squamous cell carcinoma cell lines, real-time PCR was used to measure the mRNA levels of Hsp27. Real-time PCR result showed that Hsp27 mRNA expression level was 22.4 ± 0.84 fold higher in metastatic UM-SCC-22B compared to primary UM-SCC-22A (Fig. 3b). This pair of head and neck squamous cell carcinoma cells with different Hsp27 expression levels and metastatic potential provide an excellent cell model to elucidate the possible function of Hsp27.

siRNA transfection knocks down Hsp27 mRNA and protein expression in head and neck squamous cell carcinoma cells (HNSCC)

To obtain insight into whether Hsp27 is directly linked to HNSCC cell invasion and migration ability, Hsp27 knockdown with small interference RNA (siRNA) was performed in the metastatic UM-SCC-22B cell line with high Hsp27 expression level. UM-SCC-22B cells were transfected for 24hr with 33 nM siRNA, total RNA was extracted from cells by TRIzol reagents. Real-time PCR was used to measure Hsp27 mRNA level and western blotting was used to quantify the protein level of Hsp27. Real-time PCR showed that siRNA knocked down hsp27 mRNA expression level by 83% in metastatic UM-SCC-22B compared with control (Fig. 4a). Western blotting revealed that siRNA transfection decreased hsp27 protein level 23-fold in metastatic UM-SCC-22B compared to control transfected cells (Fig. 4b). Thus silencing Hsp27 with small interfering RNA successfully reduced the expression of Hsp27 in mRNA and protein level.

Silencing Hsp27 inhibits head and neck squamous cell carcinoma cells (HNSCC) migration and invasion

To study whether silencing of Hsp27 in HNSCC could reduce invasion and migration, in vitro matrigel invasion assay and wound-healing migration assays were conducted with UM-SCC-22B after Hsp27 siRNA knock down. Cells were transfected with Hsp27 siRNA for 5 hr. For the invasion assay, 2×10^4 cells were added to the upper chamber in culture medium containing 1% FBS with medium containing 10%FBS in lower chamber. At 40 hr, the cells on the lower surface of filter were counted under microscope (Fig. 5a). Eight fields were counted in each plate. Six experiments were conducted. The results showed that the cells number of UM-SCC-22B cells invading through matrigel was 53. 6 ± 26.7 (n = 6), whereas the invading cells number of UM-SCC-22B with Hsp27 siRNA transfection was 26.9± 11.2 (n = 6) (Fig. 5b). This is comparable to the primary HNSCC, UM-SCC-22A (with rarely Hsp27 expression), which had 25.5 ±14.6 (Fig. 2b) invading cells on the lower surface of filter.

In the migration assay, after the wound gap was generated, the cells were cultured for 24–72 hr (Fig. 5c). After 24, 48, and 72 hr, the metastatic UM-SCC-22B migrated significantly faster and the gap width was reduced by 34.2±8.2%, 64.4±7.3%, 71.7 ±6.8%, respectively. In comparison, when metastatic UM-SCC-22B was transfected with Hsp27 siRNA, the gap width was reduced by only 11.6±9.0%, 13.1±3.0%, 18.3±7.9% at 24, 48, and 72 hr (Fig. 5d). Similarly, the migration ability of UM-SCC-22B with siRNA transfection is comparable to the primary HNSCC, UM-SCC-22A (with rarely Hsp27 expression) (Fig. 2d). These data suggest that silencing Hsp27 in the metastatic cell line indeed diminishes the motility and invasion of UM-SCC-22B.

Discussion

The small Heat Shock Protein 27 (Hsp27) belongs to heat shock protein family, and acts as a molecular chaperone. Hsp27 is localized in the cytosol of most human cells at a low level 27. Expression of Hsp27 can be induced by environmental stress, such as heat shock, heavy metals, oxidants, infection, inflammation, ischemia28, 29. Once Hsp27 is induced, it may be phosphorylated and translocated from cytoplasm into or around the nucleus 30–32. Hsp27 has been shown to have various cellular functions to promote differentiation, proliferation 29, cell growth, and motility 17. In addition, it has been reported that Hsp27 is associated with various carcinomas. However, studies showed that Hsp27 is overexpressed in some cancer types, but downregulated in others 33, 34. Increased levels of Hsp27 was detected in various cancers, such as breast 35, 36, endometrial 37, prostate 38 14, ovarian 39, oral squamous cell 29, gastric 40, 41, and liver cancer 42, in these cancer types, Hsp27 is

considered to be a negative prognostic factor. A recent study identified 16 proteins associated with primary hepatocellular carcinoma (HCC) with or without metastases 15. Among these proteins, Hsp27 was found to be correlated with HCC metastasis. Therefore, overexpression of Hsp27 serves as a unique feature of metastatic HCC. In addition, higher levels of hsp27 expression is also considered to be associated with invasion and metastasis in tongue squamous cell cancer 22.

On the other hand, Hsp27 has also been reported to be a good prognosis indicator. In patients with malignant fibrous histiocytoma 19, neuroblastoma 43, endometrial adenocarcinomas 37, 44 and oesophageal cancer 23, 45, high levels of Hsp27 have been correlated with good prognosis. Masanobu N et al. 23 showed that patients with Hsp27-negative esophageal squamous cell carcinoma tended to have a poor prognosis compared with patients with Hsp27-positive tumors. Hsp27 did not correlate with cancer and metastasis in renal cell carcinoma 17.

To date, Hsp27 has not been conclusively studied in head and neck squamous cell cancers. Our data indicates that a higher level of Hsp27 is a negative prognostic factor. We found that Hsp27 is overexpressed in a human head and neck squamous cell cancer cells with high metastatic ability.

Since cancer and its metastasis are complex processes, various cancer types and their metastasis processes have different oncogenic pathways involved 18. Different cancers may have distinct biomarker signatures that contribute their metastatic behavior. Literature report that the process of metastasis is regulated by a variety of internal and external signals via complex signal transduction cascades. A variety of molecules including FAK, Src, MMPs, Her-2, and actin cytoskeleton 46 are involved in cell migration. Our data indeed showed that primary cancer cells (22A) still express these proteins (such as Her-2, data not shown). Although two different cell lines with different metastasis ability show dramatic difference in Hsp27 expression, , we can not rule out the contribution of the other molecular for metastasis. Therefore, the expression levels of Hsp27 is only one of the reasons to manifest migratory behavior for 22A. In addition, it is also not surprising that Hsp27 may play different roles in different cancer types. And thus it is rather challenging to compare Hsp27 function in different cancer types.

To simplify the model, we selected a pair of head and neck cell lines from the same patient, but with different metastastic potential to dissect the functions of Hsp27. This pair of cell lines will limit individual difference and minimize the genetic variation. The cancer cell lines were isolated from surgical specimens of a previously untreated patient with a primary tumor in the throat and a metastatic lymph node in the neck. The present study using these two cell lines from the same patient provides excellent model to study function of Hsp27 in metastasis without other interference. In these two cell lines from the same patient, we monitored the cell migration and invasion ability, Hsp27 expression levels, siRNA knockdown of Hsp27. Indeed, the metastatic head and neck squamous cell cancer cell line UM-SCC-22B has higher invasion and migration ability compared to the primary squamous cell cancer cell line UM-SCC-22A,, although these two cell lines have similar proliferation rate. Furthermore, Hsp27 is overexpressed in the metastatic UM-SCC-22B, but is rarely detectable in the primary UM-SCC22A. Silencing Hsp27 by siRNA in metastatic UM-SCC-22B cells reduced its invasion and migration ability to levels similar to that of the primary cancer cells UM-SCC-22A. In this regard, detection of Hsp27 in head and neck cancers may help us understand one of the molecular mechanisms of metastasis, and provide a biomarker for the prognosis of head and neck cancer after treatment 47. It is worth noting that further clinical evaluation is warranted for validate these findings.

Acknowledgments

This work was partially supported by the National Institutes of Health (R01 CA120023 and R21 CA143474); University of Michigan Cancer Center Research Grant (Munn); and University of Michigan Cancer Center Core Grant to DS, as well as by R01 DE13346; Michigan Institute for Clinical & Health Research (MICHR) UL1RR024986 (TEC); NIH NIDCR; P30 DC05188; NCI and NIDCR Head and Neck Cancer SPORE P50 CA97248; NCI Cancer Center Support Grant P30 CA46592;. This study was also partially supported by Chinese Scholarship Council (2009) and Shandong University Oversea Study Scholarship (2008).

References

1. Kim MH, Kitson RP, Albertsson P, Nannmark U, Basse PH, Kuppen PJ, Hokland ME, Goldfarb RH. Secreted and membrane-associated matrix metalloproteinases of IL-2-activated NK cells and their inhibitors. J Immunol. 2000; 164(11):5883–5889. [PubMed: 10820269]
2. Edwards BK, Howe HL, Ries LA, Thun MJ, Rosenberg HM, Yancik R, Wingo PA, Jemal A, Feigal EG. Annual report to the nation on the status of cancer, 1973–1999, featuring implications of age and aging on U.S. cancer burden. Cancer. 2002; 94(10):2766–2792. [PubMed: 12173348]
3. Werner JA, Rathcke IO, Mandic R. The role of matrix metalloproteinases in squamous cell carcinomas of the head and neck. Clin Exp Metastasis. 2002; 19(4):275–282. [PubMed: 12090467]
4. Ginos MA, Page GP, Michalowicz BS, Patel KJ, Volker SE, Pambuccian SE, Ondrey FG, Adams GL, Gaffney PM. Identification of a gene expression signature associated with recurrent disease in squamous cell carcinoma of the head and neck. Cancer Res. 2004; 64(1):55–63. [PubMed: 14729608]
5. Tsutsumi S, Neckers L. Extracellular heat shock protein 90: a role for a molecular chaperone in cell motility and cancer metastasis. Cancer Sci. 2007; 98(10):1536–1539. [PubMed: 17645779]
6. Yoshizaki T, Maruyama Y, Sato H, Furukawa M. Expression of tissue inhibitor of matrix metalloproteinase-2 correlates with activation of matrix metalloproteinase-2 and predicts poor prognosis in tongue squamous cell carcinoma. Int J Cancer. 2001; 95(1):44–50. [PubMed: 11241310]
7. Patel BP, Shah SV, Shukla SN, Shah PM, Patel PS. Clinical significance of MMP-2 and MMP-9 in patients with oral cancer. Head Neck. 2007; 29(6):564–572. [PubMed: 17252594]
8. Dasgupta S, Bhattacharya-Chatterjee M, O'Malley BW Jr, Chatterjee SK. Tumor metastasis in an orthotopic murine model of head and neck cancer: possible role of TGF-beta 1 secreted by the tumor cells. J Cell Biochem. 2006; 97(5):1036–1051. [PubMed: 16294321]
9. Hoang AT, Huang J, Rudra-Ganguly N, Zheng J, Powell WC, Rabindran SK, Wu C, Roy-Burman P. A novel association between the human heat shock transcription factor 1 (HSF1) and prostate adenocarcinoma. Am J Pathol. 2000; 156(3):857–864. [PubMed: 10702402]
10. Calderwood SK, Khaleque MA, Sawyer DB, Ciocca DR. Heat shock proteins in cancer: chaperones of tumorigenesis. Trends Biochem Sci. 2006; 31(3):164–172. [PubMed: 16483782]
11. Ciocca DR, Calderwood SK. Heat shock proteins in cancer: diagnostic, prognostic, predictive, and treatment implications. Cell Stress Chaperones. 2005; 10(2):86–103. [PubMed: 16038406]
12. Wang Y, Theriault JR, He H, Gong J, Calderwood SK. Expression of a dominant negative heat shock factor-1 construct inhibits aneuploidy in prostate carcinoma cells. J Biol Chem. 2004; 279(31):32651–32659. [PubMed: 15152009]
13. Ciocca DR, Oesterreich S, Chamness GC, McGuire WL, Fuqua SA. Biological and clinical implications of heat shock protein 27,000 (Hsp27): a review. J Natl Cancer Inst. 1993; 85(19): 1558–1570. [PubMed: 8411230]
14. Cornford PA, Dodson AR, Parsons KF, Desmond AD, Woolfenden A, Fordham M, Neoptolemos JP, Ke Y, Foster CS. Heat shock protein expression independently predicts clinical outcome in prostate cancer. Cancer Res. 2000; 60(24):7099–7105. [PubMed: 11156417]
15. Song HY, Liu YK, Feng JT, Cui JF, Dai Z, Zhang LJ, Feng JX, Shen HL, Tang ZY. Proteomic analysis on metastasis-associated proteins of human hepatocellular carcinoma tissues. J Cancer Res Clin Oncol. 2006; 132(2):92–98. [PubMed: 16261346]

16. Guo K, Kang NX, Li Y, Sun L, Gan L, Cui FJ, Gao MD, Liu KY. Regulation of HSP27 on NF-kappaB pathway activation may be involved in metastatic hepatocellular carcinoma cells apoptosis. BMC Cancer. 2009; 9:100. [PubMed: 19331697]

17. Erkizan O, Kirkali G, Yorukoglu K, Kirkali Z. Significance of heat shock protein-27 expression in patients with renal cell carcinoma. Urology. 2004; 64(3):474–478. [PubMed: 15351573]

18. Wang A, Liu X, Sheng S, Ye H, Peng T, Shi F, Crowe DL, Zhou X. Dysregulation of heat shock protein 27 expression in oral tongue squamous cell carcinoma. BMC Cancer. 2009; 9:167. [PubMed: 19497117]

19. Tetu B, Lacasse B, Bouchard HL, Lagace R, Huot J, Landry J. Prognostic influence of HSP-27 expression in malignant fibrous histiocytoma: a clinicopathological and immunohistochemical study. Cancer Res. 1992; 52(8):2325–2328. [PubMed: 1313743]

20. Garrido C, Fromentin A, Bonnotte B, Favre N, Moutet M, Arrigo AP, Mehlen P, Solary E. Heat shock protein 27 enhances the tumorigenicity of immunogenic rat colon carcinoma cell clones. Cancer Res. 1998; 58(23):5495–5499. [PubMed: 9850085]

21. Bruey JM, Paul C, Fromentin A, Hilpert S, Arrigo AP, Solary E, Garrido C. Differential regulation of HSP27 oligomerization in tumor cells grown in vitro and in vivo. Oncogene. 2000; 19(42): 4855–4863. [PubMed: 11039903]

22. Ye H, Wang A, Lee BS, Yu T, Sheng S, Peng T, Hu S, Crowe DL, Zhou X. Proteomic based identification of manganese superoxide dismutase 2 (SOD2) as a metastasis marker for oral squamous cell carcinoma. Cancer Genomics Proteomics. 2008; 5(2):85–94. [PubMed: 18460737]

23. Nakajima M, Kuwano H, Miyazaki T, Masuda N, Kato H. Significant correlation between expression of heat shock proteins 27, 70 and lymphocyte infiltration in esophageal squamous cell carcinoma. Cancer Lett. 2002; 178(1):99–106. [PubMed: 11849747]

24. Cao X, Bloomston M, Zhang T, Frankel WL, Jia G, Wang B, Hall NC, Koch RM, Cheng H, Knopp MV, Sun D. Synergistic antipancreatic tumor effect by simultaneously targeting hypoxic cancer cells with HSP90 inhibitor and glycolysis inhibitor. Clin Cancer Res. 2008; 14(6):1831–1839. [PubMed: 18347186]

25. McCollum AK, Teneyck CJ, Sauer BM, Toft DO, Erlichman C. Up-regulation of heat shock protein 27 induces resistance to 17-allylamino-demethoxygeldanamycin through a glutathione-mediated mechanism. Cancer Res. 2006; 66(22):10967–10975. [PubMed: 17108135]

26. Zhang X, Chen ZG, Choe MS, Lin Y, Sun SY, Wieand HS, Shin HJ, Chen A, Khuri FR, Shin DM. Tumor growth inhibition by simultaneously blocking epidermal growth factor receptor and cyclooxygenase-2 in a xenograft model. Clin Cancer Res. 2005; 11(17):6261–6269. [PubMed: 16144930]

27. Lindquist S, Craig EA. The heat-shock proteins. Annu Rev Genet. 1988; 22:631–677. [PubMed: 2853609]

28. Lichtenfels R, Kellner R, Bukur J, Beck J, Brenner W, Ackermann A, Seliger B. Heat shock protein expression and anti-heat shock protein reactivity in renal cell carcinoma. Proteomics. 2002; 2(5):561–570. [PubMed: 11987130]

29. Mese H, Sasaki A, Nakayama S, Yoshioka N, Yoshihama Y, Kishimoto K, Matsumura T. Prognostic significance of heat shock protein 27 (HSP27) in patients with oral squamous cell carcinoma. Oncol Rep. 2002; 9(2):341–344. [PubMed: 11836604]

30. Lavoie JN, Gingras-Breton G, Tanguay RM, Landry J. Induction of Chinese hamster HSP27 gene expression in mouse cells confers resistance to heat shock. HSP27 stabilization of the microfilament organization. J Biol Chem. 1993; 268(5):3420–3429. [PubMed: 8429018]

31. Arrigo AP, Suhan JP, Welch WJ. Dynamic changes in the structure and intracellular locale of the mammalian low-molecular-weight heat shock protein. Mol Cell Biol. 1988; 8(12):5059–5071. [PubMed: 3072471]

32. Landry J, Chretien P, Laszlo A, Lambert H. Phosphorylation of HSP27 during development and decay of thermotolerance in Chinese hamster cells. J Cell Physiol. 1991; 147(1):93–101. [PubMed: 2037626]

33. Ciocca DR, Adams DJ, Edwards DP, Bjercke RJ, McGuire WL. Distribution of an estrogen-induced protein with a molecular weight of 24,000 in normal and malignant human tissues and cells. Cancer Res. 1983; 43(3):1204–1210. [PubMed: 6825091]

34. Ferrarini M, Heltai S, Zocchi MR, Rugarli C. Unusual expression and localization of heat-shock proteins in human tumor cells. Int J Cancer. 1992; 51(4):613–619. [PubMed: 1601523]
35. Thor A, Benz C, Moore D 2nd, Goldman E, Edgerton S, Landry J, Schwartz L, Mayall B, Hickey E, Weber LA. Stress response protein (srp-27) determination in primary human breast carcinomas: clinical, histologic, and prognostic correlations. J Natl Cancer Inst. 1991; 83(3):170–178. [PubMed: 1988702]
36. Storm FK, Mahvi DM, Gilchrist KW. Heat shock protein 27 overexpression in breast cancer lymph node metastasis. Ann Surg Oncol. 1996; 3(6):570–573. [PubMed: 8915490]
37. Geisler JP, Geisler HE, Tammela J, Miller GA, Wiemann MC, Zhou Z. A study of heat shock protein 27 in endometrial carcinoma. Gynecol Oncol. 1999; 72(3):347–350. [PubMed: 10053106]
38. Bonkhoff H, Fixemer T, Hunsicker I, Remberger K. Estrogen receptor gene expression and its relation to the estrogen-inducible HSP27 heat shock protein in hormone refractory prostate cancer. Prostate. 2000; 45(1):36–41. [PubMed: 10960840]
39. Arts HJ, Hollema H, Lemstra W, Willemse PH, De Vries EG, Kampinga HH, Van der Zee AG. Heat-shock-protein-27 (hsp27) expression in ovarian carcinoma: relation in response to chemotherapy and prognosis. Int J Cancer. 1999; 84(3):234–238. [PubMed: 10371339]
40. Kapranos N, Kominea A, Konstantinopoulos PA, Savva S, Artelaris S, Vandoros G, Sotiropoulou-Bonikou G, Papavassiliou AG. Expression of the 27-kDa heat shock protein (HSP27) in gastric carcinomas and adjacent normal, metaplastic, and dysplastic gastric mucosa, and its prognostic significance. J Cancer Res Clin Oncol. 2002; 128(8):426–432. [PubMed: 12200599]
41. Takeno S, Noguchi T, Kikuchi R, Sato T, Uchida Y, Yokoyama S. Analysis of the survival period in resectable stage IV gastric cancer. Ann Surg Oncol. 2001; 8(3):215–221. [PubMed: 11314937]
42. King KL, Li AF, Chau GY, Chi CW, Wu CW, Huang CL, Lui WY. Prognostic significance of heat shock protein-27 expression in hepatocellular carcinoma and its relation to histologic grading and survival. Cancer. 2000; 88(11):2464–2470. [PubMed: 10861421]
43. Ungar DR, Hailat N, Strahler JR, Kuick RD, Brodeur GM, Seeger RC, Reynolds CP, Hanash SM. Hsp27 expression in neuroblastoma: correlation with disease stage. J Natl Cancer Inst. 1994; 86(10):780–784. [PubMed: 8169976]
44. Piura B, Rabinovich A, Yavelsky V, Wolfson M. Heat shock proteins and malignancies of the female genital tract. Harefuah. 2002; 141(11):969–972. 1010, 1009. [PubMed: 12476632]
45. Kawanishi K, Shiozaki H, Doki Y, Sakita I, Inoue M, Yano M, Tsujinaka T, Shamma A, Monden M. Prognostic significance of heat shock proteins 27 and 70 in patients with squamous cell carcinoma of the esophagus. Cancer. 1999; 85(8):1649–1657. [PubMed: 10223556]
46. Dormann D, Weijer CJ. Imaging of cell migration. EMBO J. 2006; 25(15):3480–3493. [PubMed: 16900100]
47. He QY, Chen J, Kung HF, Yuen AP, Chiu JF. Identification of tumor-associated proteins in oral tongue squamous cell carcinoma by proteomics. Proteomics. 2004; 4(1):271–278. [PubMed: 14730689]

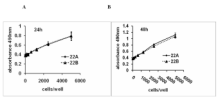

Figure 1.
Growth rate of UM-SCC-22A and UM-SCC-22B. Various numbers of UM-SCC22A and UM-SCC22B cells were seeded in 96-well plate, cultured for 24/48hr. MTS was used to measure the cell proliferation. Each point represents the mean± SD of 3 replicates. The correlation indicating a linear response between cell number and absorbance at 490nm. The background absorbance shown at zero cells/well was subtracted from these data.

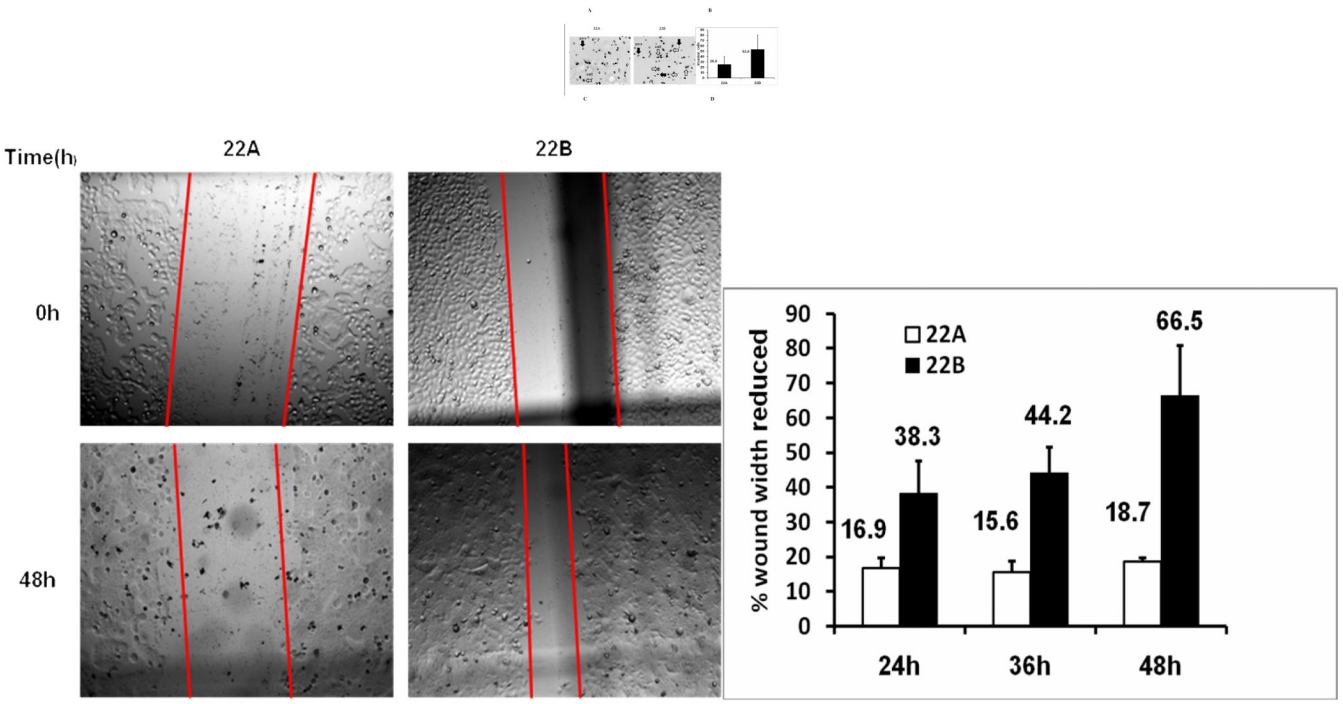

Figure 2.

Cell invasion and migration of UM-SCC-22A and UM-SCC-22B. A. Microscopy image (×100) of invading cells in Matrigel filter invasion assay from one representative experiment. Open arrows, pore; Solid arrows, cell. In the fields shown, 9 cells are apparent in the UM-SCC-22A culture and 16 are apparent in the UM-SCC-22B culture. B. Bar graph represents invading cells number (mean ± SD) of UM-SCC22A and UM-SCC22B. from six cell invasion experiments. (*p< 0.01). C. Microscopy image (×40) of cell migration of UM-SCC-22A and UM-SCC-22B from one representative experiment. D. Bar graph represents the percentage of reduced wound width (%) compared to time 0 of UM-SCC-22A and UM-SCC-22B. from six cell migration experiments. Blank bar, UM-SCC-22A; filled bar, UM-SCC-22B.

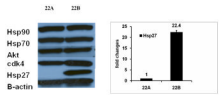

Figure 3.

A. Western blotting to detect protein levels of molecular chaperones and oncogenic proteins in UM-SCC-22A and UM-SCC-22B. The cells were lysed, and the soluble protein (35ug protein per lane) was separated by SDS-PAGE and detected by western blotting using the specific antibodies. β-actin was used as control for protein loading. B. Real-Time PCR to detect the Hsp27 mRNA level in UM-SCC-22A and UM-SCC-22B. Fold change was calculated by $2^{-\Delta\Delta ct}$.

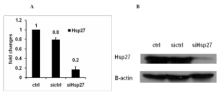

Figure 4.

A. Real-time PCR to detect Hsp27 mRNA level in UM-SCC-22B cells after siRNA transfection. SiHsp27, transfected with siRNA of Hsp27. Ctrl, cell treated with transfection reagents lipofectamine 2000; Sictrl: cells transfected with scrambled siRNA. B. Western blotting to detect protein levels of Hsp27 in UM-SCC-22B cells after siRNA transfection. The cells were transfected with scrambled siRNA (sictrl) or Hsp27 siRNA (siHsp27) for 48hr. The resulting cells were lysed, and the soluble protein (35ug protein per lane) was separated by SDS-PAGE and detected by western blotting using the specific antibodies. β-actin was used as control for protein loading.

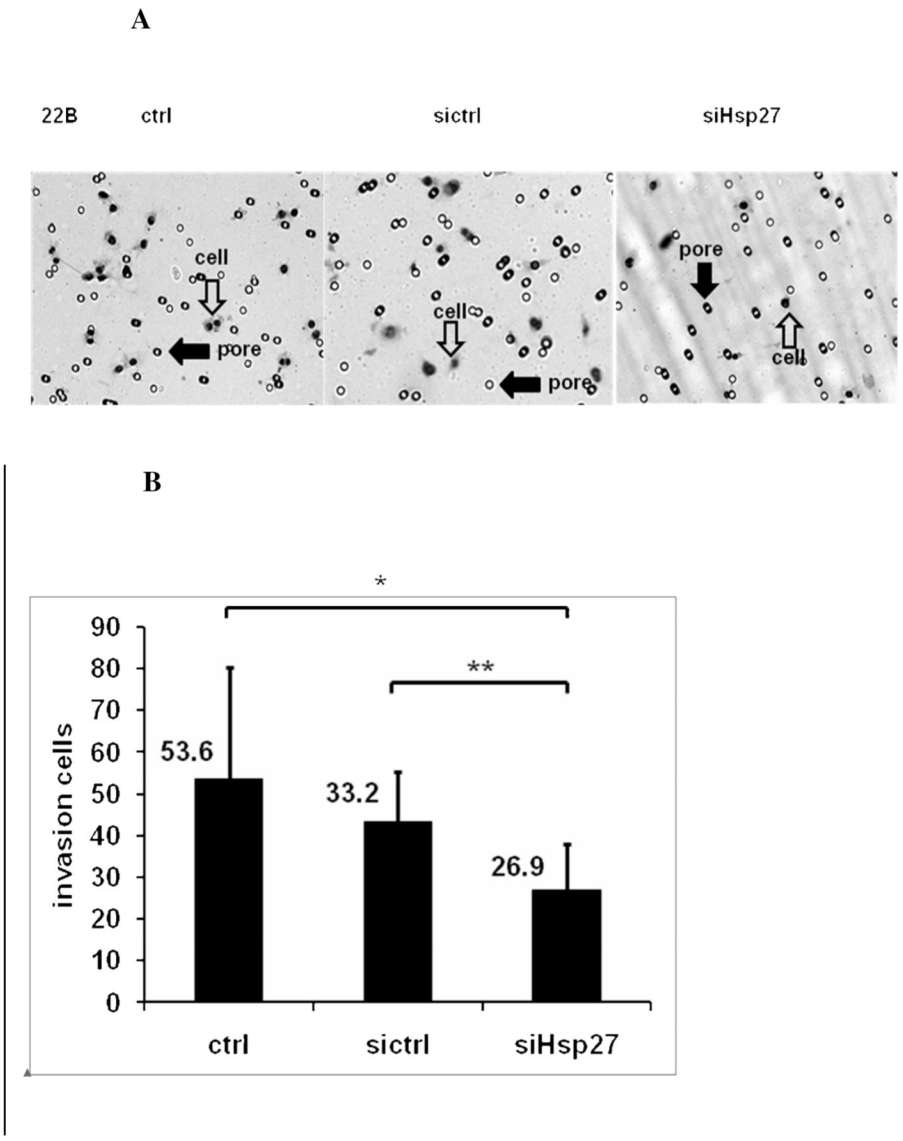

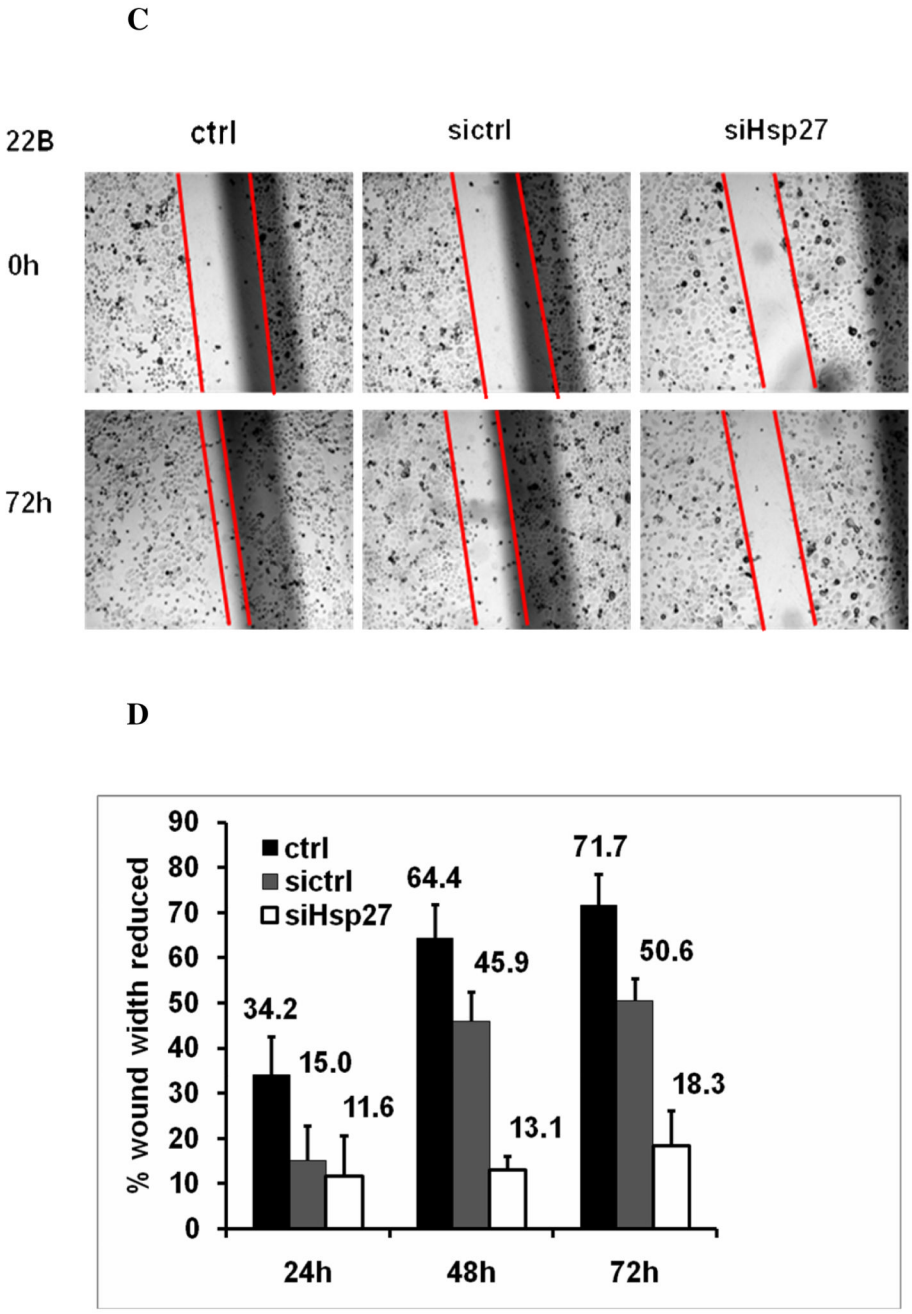

Figure 5.

A. Microscopy image (×100) of cell invasion in UM-SCC-22B after siRNA transfection in one representative experiment. Ctrl, cells treated with transfection reagents lipofectamine 2000; Sictrl: cells transfected with scrambled siRNA, SiHsp27, cells transfected with siRNA of Hsp27; Open arrows: pore; Solid arrows: cell. B. Bar graph represents a summary of six experiments of invading numbers of UM-SCC-22B cells after transfection with siHsp27, or control siRNA. X ±SD (n=6). UM-SCC-22B cells treated with 33nM Hsp27 siRNA have a 49.76% (*p< 0.01) reduction in cell invasion compared to control cells and 18.99% (**p< 0.01) relative to control siRNA treated UM-SCC-22B cells. Ctrl, cells treated with transfection reagent lipofectamine 2000; Sictrl: cells transfected with scrambled siRNA,

SiHsp27, transfected with Hsp27 siRNA. C. Microscopy image (×40) of cell migration of UM-SCC-22B after siRNA transfection in one representative experiment. Ctrl, cell treated with transfection reagent lipofectamine 2000; Sictrl: cells transfected with scrambled siRNA; SiHsp27 transfected with Hsp27 siRNA. D. Bar graph represents the percentage of reduced wound width (%) after 24–72 hr in UM-SCC-22B cells after siRNA transfection. Ctrl: cells treated with transfection reagent lipofectamine 2000; Sictrl: cells transfected with scrambled siRNA: SiHsp27: transfected with siRNA of Hsp27.